***Journal of Nanoparticle Research 19* (2017) 181**

DOI 10.1007/s11051-017-3876-9
https://link.springer.com/article/10.1007/s11051-017-3876-9

DNA-Assisted Decoration of Single-Walled Carbon Nanotubes with Gold Nanoparticles for Applications in Surface Enhanced Raman Scattering Imaging of Cells

Elena-Laura Ursu, Florica Doroftei, Dragos Peptanariu, Mariana Pinteala and Alexandru Rotaru*

"Petru Poni" Institute of Macromolecular Chemistry, Romanian Academy
Centre of Advanced Research in Bionanoconjugates and Biopolymers
Aleea Grigore Ghica Voda 41 A, 700487 Iasi, Romania.
e-mail: rotaru.alexandru@icmpp.ro
telephone: +40 232 217454
fax: +40 232 211 299

Abstract

Single-walled carbon nanotubes (SWNTs) are 1D nanostructures with distinct physical and chemical properties that have shown great promise for applications in many fields, including biomedicine. Since for biomedical application the water solubility is crucial and SWNTs have low solubility, various methods (including polymer and biopolymer wrapping, chemical modifications) have been developed to solubilize and disperse them in water. Due to their unique optical properties such as photoluminescence in the NIR and strong resonant Raman signatures, they can be used as nanoprobes in biomedical imaging and phototherapies. Furthermore, decoration of SWNTs with noble metal nanoparticles will induce an excellent surface-enhanced Raman scattering (SERS) effect of the nanoparticles-SWNTs composites, with applications in cell imaging. Herein, we present a new and facile strategy for the DNA-assisted decoration of SWNTs with gold nanoparticles (AuNPs) and their application in SERS imaging. By ultrasonication at room temperature of SWNTs with AuNPs functionalized with synthetic DNA, SWNT-AuNPs nanocomposites with enhanced Raman signal were obtained. Among the important advantages of the proposed method are the presence of the free DNA overhangs around the SWNT-AuNPs suitable for post-synthetic modification of nanocomposite through hybridization of complementary DNA strands containing molecules of interest attached by well-developed bio-conjugation chemistry.

Introduction

Singe-walled carbon nanotubes (SWNTs), have attracted significant interest in the area of bio-oriented medicine, for potential applications in biological detection, drug delivery, phototherapies, and biomedical imaging (Liu et al. 2011; Liu et al. 2011; Yang et al. 2010; Kam et al. 2005; Liu et al. 2008; Bartelmess et al. 2015). These particular applications owe to the unique one-dimensional structure of SWNTs which exhibit distinctive resonance-enhanced Raman signatures for Raman detection/imaging (Heller et al. 2005; Rao et al. 1997). Since the first report on Raman imaging of SWNTs in live cells by Heller et al. in 2005, the field has gained a continuous attention (Bartelmess et al. 2015). Despite the great focus towards the field, applications of pristine SWNTs are still limited by a relatively low molar extinction coefficient (4.4×10^3 M^{-1} cm^{-1}) (Schoeppler et al. 2011) and thus relatively long spectral acquisition time. Surface enhanced Raman scattering (SERS) is an effect able to strongly enhance Raman signals of molecules close to the noble metal surfaces or nanoparticles by as high as many orders of magnitude (Qian et al. 2008; Cao et al. 2002; Zavaleta et al. 2009). SERS with SWNTs studies and biomedical applications have also been widely investigated in recent years (Krafft et al. 2016; Bartelmess et al 2015; Chen et al 2008; Beqa et al. 2011). Since the pristine SWNTs have no functional binding groups apart from some carboxyl groups on the defect sites and the tube-ends, it is still a challenge to develop a facile method for the uniform functionalization of carbon nanotubes with metal nanoparticles suitable for biomedical imaging. Several interesting routes have now been known and devised for either covalently or noncovalent attaching of certain metal nanoparticles onto carbon nanotubes (Moghaddam et al. 2004; Quinn et al. 2005; Chu et al. 2010; Choi et al. 2002; Azamian et al. 2002). The noncovalent approach is in advantage by maintaining the properties of the nanotube, the carbon scaffold being minimally perturbed during the functionalization. Even though a variety of methods have been demonstrated for the noncovalent decoration of SWNTs with metal nanoparticles, we observed some impediments in fabrication of water-soluble, functional and dispersed SWNT/noble metal hybrid materials suitable for biomedical SERS imaging. Biopolymers could represent a solution to some of the existing problems and several interesting techniques have already been reported, involving the use of biopolymers for the preparation of SWNTs-metal nanocomposites. Lu and co-workers (Meng et al. 2014) have described a subtle method for the synthesis of golden SWNTs nanohybrids by using the layer by layer self-assembly of two oppositely charged polysaccharides on SWNTs as bridge, followed by the deposited of gold nanoparticles (AuNPs) on the SWNT surface by an in situ reduction approach. Earlier, Deng and co-workers have extensively used different DNA designs, including thiol-modified DNA sequences (Han et al. 2007) or hybridizable DNA sequences (Li et al. 2007) wrapped around SWNT to efficiently attach AuNPs. Towards the use of DNA, Liu and co-workers (Wang et al. 2012) reported an interesting and facile in situ solution phase approach to grow noble metal nanoparticles onto noncovalently dispersed SWNTs stabilized by DNA with the

subsequent functionalization for targeted delivery. The authors succeeded in obtaining final SWNT-metal nanoparticles-PEG nanocomposites with successful application in SERS imaging of cells. Still, some of the above presented strategies require quit a number of synthetic steps, and do not offer too many facile possibilities in controlling neither the exact size of the decorated nanoparticles nor the incorporation of specific targeting molecules to the final nanocomposite. Here, we report a simplified, DNA-assisted method for the preparation of SWNT-AuNPs composites (Fig. 1) which, due to the excess of free DNA overhangs around starting AuNPs, could be subsequently functionalized with molecules of interest by means of hybridization with a labeled complementary DNA strand.

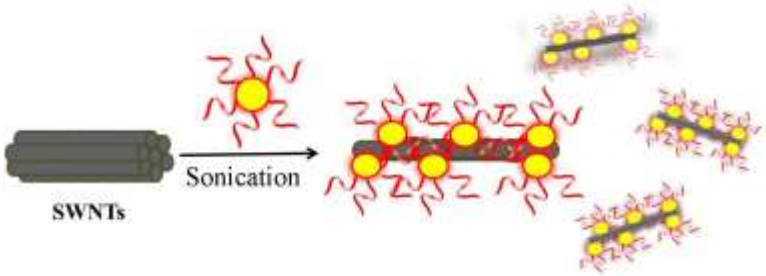

Fig. 1 Schematic illustration for the fabrication of water-soluble SWNT-AuNPs nanocomposites starting from the DNA-functionalized gold nanoparticles and pristine single-walled carbon nanotubes.

By utilizing an adapted synthetic strategy (Pal et al. 2013), we first synthesized the DNA-functionalized AuNPs which, after a purification step, were used directly to disperse the pristine SWNTs utilizing ultrasonication. The sonication time was carefully varied to prepare optimum SWNT-AuNPs nanocomposites, the process being monitored by atomic force microscopy (AFM), transition electron microscopy (TEM) and by the enhancement of SWNTs SERS signal. The optimal SWNT-AuNPs nanocomposites were tested for the SERS imaging of HeLa cells and for hybridization experiments to check the possibility for the post-synthetic attachment of DNA-conjugated molecules of interest. The proposed approach holds promise as a variable platform for the preparation of water soluble SWNT-AuNPs nanostructures with the possibility of post-synthetic functionalization with organic ligands through the complementary strand hybridization of the corresponding DNA conjugates.

Experimental

Reagents

Gold(III) chloride hydrate, trisodium citrate, bis(*p*-sulfonatophenyl)phenylphosphine dehydrate dipotassium salt, sodium chloride, magnesium cloride, methanol and SWNT® SG 76 single-wall carbon nanotubes were purchased from Sigma Aldrich (Munich, Germany). 10xTAE buffer was purchased from AppliChem GmbH (Germany). All DNA oligos were purchased HPLC-purified, freeze-dried from Metabion AG (Germany) and diluted to the concentration of 100 µL. HeLa (human

cervix adenocarcinoma) cells from CLS-Cell-Lines-Services-GmbH, Germany were propagated in *alpha*-MEM medium (Lonza) supplemented with 10% fetal bovine serum (FBS, Gibco) and 1% penicillin–streptomycin–amphotericin B mixture (Lonza) in a 37°C, 5% CO_2 humidified environment. Ultrapure water was used for preparing the working solutions in all the experiments.

Preparation of DNA-functionalized AuNPs

The detailed experimental conditions for the preparation and subsequent functionalization of AuNPs are described in supplementary materials. Thus, citrate coated AuNPs (20 nm) were synthesized using an adapted Turkevich method (Turkevich et al. 1951; Potle et al. 2010). Phosphine coated AuNPs were synthesized following well-established strategy based on previous reports (Pal et al. 2013; Ding et al. 2010). In order to cover the AuNPs with DNA, the phosphine coated AuNPs with an excess of approximately 200 fold of thiol modified DNA (5'-$(T)_{40}$-SH-3') were gently mixed for 48 hours. To remove the excess of unbound DNA, the mixture was purified using Amiconcon centrifugal filter Ultrace-100K devices (100,000 NMWL, purchased from Millipore, catalogue number: UFC510096), following the standard washing procedure recommended by the supplier, using 1xTAE buffer (pH = 7.4).

Preparation of CNT-AuNPs conjugates

To deposit AuNPs on SWNT, a suspension of SWNTs in ultrapure water (1 mg SWNTs in 1 mL H2O) was prepared. From this sonicated stock solution, 1, 3 or 5 µL were mixed together with the filtered DNA-functionalized AuNPs (40µL, 1µM) and 10xTAE buffer (5µL) to the final volume of 50 µL. The obtained suspension was sonicated in a water/ice bath on VWR ultrasonic bath from 0 to 150 minutes in order to obtain dark-red SWNT-AuNPs mixtures. Thus prepared mixtures were subsequently used for characterization, Raman analysis and cell transfection experiments.

DNA hybridization experiments

TAMRA-labeled DNA sequences 5'-TAMRA-$(A)_{40}$-3' (positive control) and 5'-TAMRA-$(C)_{40}$-3' (negative control) were dissolved separately in 1xTAE buffer (pH = 7.4) and NaCl (0.1 M) to the final volume of 500 µL. The emission spectra of the solution were measured by exciting at 557 nm on a Fluoromax 4 (Horiba Scientific) fluorescence spectrophotometer. Next, to the investigated solutions a fixed amount of freshly prepared SWNT-AuNPs solution (5 µL) was added and the emission was measured after 0, 30, 60, 120 and 180 min.

Characterisation techniques

UV/vis spectra were obtained with a PerkinElmer Lambda 35 UV/vis spectrophotometer (wavelength range 200−1000 nm). Fluorescence spectra were acquired on a Fluoromax 4 (Horiba Scientific) fluorescence spectrophotometer using cuvettes with a sample volume of 1000 µL. The samples for atomic force microscope (AFM) analysis were deposited on freshly cleaved mica, pretreated with $MgCl_2$ solution (100 µM) for the better adhesion of DNA-functionalized samples. After drying, AFM images were recorded in air in a tapping mode using NTEGRA Spectra (NT-MDT, Russia) instrument with 3.1-37.6 N/m force constant cantilever of a silicon nitride cantilevers (NSC10, NT-MDT, Russia). Transmission electron microscopy (TEM) images were obtained using Hitachi HT7700 microscope operating at 100 kV in High Resolution Mode. TEM samples (3 µL) were deposited on 300 mesh carbon-coated copper grids and dried overnight before examination. Raman spectra for SWNT samples were recorded using a Raman spectrometer (inVia, Renishaw) in the solution phase.

Cytotoxicity test and Raman imaging of Cells

Cytotoxicity was measured using the CellTiter 96® Aqueous One Solution Cell Proliferation Assay (Promega) following manufacturer protocol. HeLa cells were seeded at a density of 10^4 cells per well in 96 well plates, in complete medium. The next day, cells were treated with the freshly-prepared SWNT-AuNPs reaction mixture (5, 10 and 20 µL of SWNT-AuNPs in 200 µL of medium) and then grown for another 24 hours. Next, 20 µL of CellTiter 96® Aqueous One Solution reagent were added to each well, and the plates were incubated for another 4 hours before reading the result. Absorbance at 490 nm was recorded with a plate reader (EnSight, PerkinElmer). Cell viability was calculated and expressed as percentage relative to viability of untreated cells. Experiments were performed in two duplicates and repeated two times. Data is presented as mean±S.D. (n=4).

Twenty four hours prior transfection, HeLa cells were plated in chamber slides with 8 wells (Lab Tek) at a density of 10^4 cells/well and allowed to attach overnight. Cells were treated with the freshly-prepared SWNT-AuNPs reaction mixture (5 µL of SWNT-AuNPs in 200 µL of medium) and after 24 hours, they were fixed with 2.5% glutaraldehyde for 15 minutes and imaged under a Raman confocal microscope (inVia, Renishaw) with a 633 nm laser (17 mW) as the excitation light source. A 50× objective lens was used and each Raman spectroscopic map contained at least 90 × 90 spectra, with 1 s integration time for each spectrum.

Results and discussions

Optimization of SWNT-AuNPs preparation

To increase the concentration of the AuNPs stock solution, 20 nm citrate-coated AuNPs obtained using the standard Turkievich method were subjected to the concentration and subsequent dispersion and

stabilization with bis(*p*-sulfonatophenyl)phenylphosphine dihydrate dipotassium salt (Ding et al. 2010). This procedure allowed us to obtain a stock solution of phosphine-stabilized AuNPs characterized by TEM (Fig. S1) equal to 1 µM which was subsequently used for the functionalization with DNA. To fully cover the surface of AuNPs with single-stranded DNA, 3'-thiol-modified-$(T)_{40}$ DNA sequence was used in a 200 fold excess, incubated at room temperature in a 1xTAE buffer solution in course of 48 hours. Subsequently, to remove the excess of unbound DNA, the reaction was filtered and washed three times with 1xTAE buffer using Amiconcon centrifugal filter Ultrace-100K devices. Thus obtained DNA-functionalized AuNPs (AuNPs-DNA) were characterized by TEM (Fig. S2) and used for the functionalization of SWNTs. In the next step, raw SWNTs (1, 3 and 5 µL) were mixed together with a fixed amount of AuNPs-DNA in 1xTAE buffer and sonicated in a conventional VWR ultrasonic bath. We expected that during the sonication a part of long single-stranded DNA sequences attached to AuNPs will wrap around the SWNTs, leading on one hand to the SWNTs dispersion and, to the attachment of AuNPs to the carbon scaffold. Aliquots from the sonicated reaction mixture were collected every 30 min and the Raman signal enhancement was monitored by measuring the spectra under 633 nm laser excitation. Particularly, the G-band peak at ~1590 cm^{-1} was observed, being the most intense Raman feature of SWNTs, also used as a direct measure for the SWNT distribution inside the biological samples. We could observe that when using 1 or 3 µL of SWNTs stock solution, very weak or no significant Raman signal or SERS effect of the investigating reactions were observed. The reaction mixture containing 5 µL of SWNTs presented a very weak Raman signal (Fig. 2, black curve) before sonication, showing a considerable Raman signal enhancement already after 30 minutes of sonication (Fig. 2, red curve).

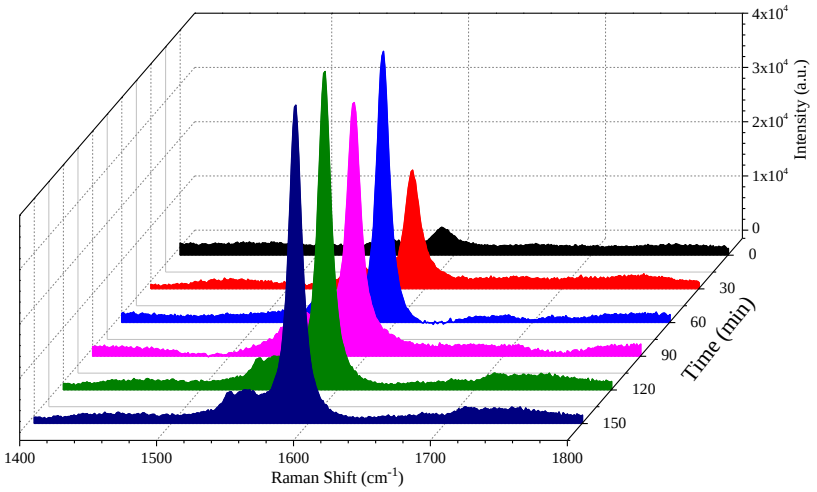

Fig. 2 Dependence of the Raman signals intensity of SWNT-AuNPs on sonication time.

The SERS enhancement effect first rose with the increase of sonication time, reaching its optimum after 60 min (Fig. 2, red and light-blue curves). Subsequent sonication did not show any Raman signal enhancement up to 150 min, meaning that the optimal sonication time for the preparation of these

nanocomposites at the utilized concentration was equal to 60 min. The SERS enhancement factor after 60 min was calculated to be ~13 (Camargo et al. 2010).

The reaction mixture after 60 min of sonication was analyzed by AFM on freshly cleaved mica, pretreated with $MgCl_2$ for better attachment of DNA modified nanoparticles or nanostructures (Fig. 3).

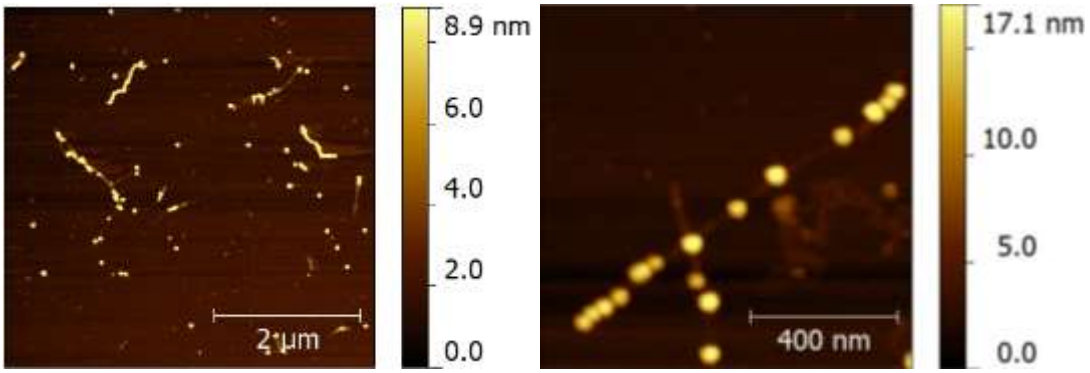

Fig. 3 Examples of AFM images of the SWNT-AuNPs after 60 min sonication.

Analyzing the AFM images, we could observe that after 60 min of continuous sonication AuNPs were attached to the carbon nanotubes yielding dispersed SWNT-AuNPs nanocomposites. Interestingly, at this ratio between SWNTs (5 µL) and AuNPs (40 µL) after careful analyses of several areas of the same mica surface (Fig. 2, S3 (A)), we did not observe large amounts of individual unbound AuNPs, meaning that at this ration between AuNPs-DNA and SWNTs the reaction is shifted towards the formation of final assemblies. TEM analysis was also employed for the characterization of the prepared nanocomposites (Fig. S4), proving the attachment of AuNPs to the SWNTs. The detailed interpretation of the TEM results was impeded by the low contrast of dispersed SWNTs, and the agglomeration of SWNT-AuNPs nanocomposites during sample preparation. Nevertheless, analyzing numerous TEM images, we could still observe multiple AuNPs aligned along SWNTs, similar to the structures observed by AFM.

Combination of AFM and Raman techniques were also employed to investigate the formation SWNT-AuNPs at higher concentration of row SWNTs. When increasing the amount of SWNTs to 10 µL or higher under standard reaction condition, we could observe an initial enhancement of the Raman signal intensity after 60 min of sonication similar to the previous experiment, followed by a strong decrease after 90 min (data not presented). This fact could be explained by the localized agglomeration of the multiple SWNTs around AuNPs which served as nucleation centers, due to the large excess of the attached single-stranded DNA overhangs, for the excess of SWNTs. This fact was proved by the AFM analyses of the sample sonicated for 90 min (Fig. S3), the results showing the appearance of multiple micrometer size agglomerations on the mica surface after 90 min of sonication. Interestingly, bulky and non-uniform agglomerations of different size were also observed by the optical microscope

when performing Raman measurements on samples after 90 min of sonication at the mentioned concentration.

RAMAN imaging of Cells

Cell toxicity test was carried out first to determine the cytotoxicity of the synthesized SWNT-AuNPs nanocomposites at optimum conditions prior to cell transfection experiments. The obtained experimental results revealed a cell viability higher than 75% at all tested concentrations (Fig. S5). Next, HeLa cells were incubated with freshly prepared SWNT-AuNPs for 24 hours, washed extensively with ultrapure water and afterwards fixed with 2.5% glutaraldehyde prior to Raman imaging (Fig. 4). The imaging was conducted using a 633 nm laser (17 mW) as the excitation light source. Additionally, an optical microscope equipped with 50× objective lens was used to compare the optical and Raman image of the investigated area.

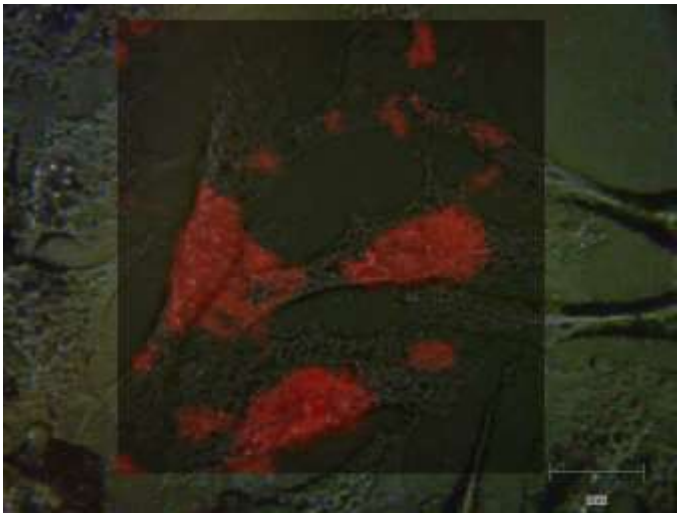

Fig. 4 Overlapped optical and Raman images of HeLa cells incubated with AuNPs-CNT for 24 hours at 37°C.

Under these experimental conditions, strong Raman signals were observed and, the recorded red areas in the Fig. 4 corresponded to G-band intensities that can be used as an indicator of the SWNT-AuNPs composites presence in the analysed cells. By overlapping optical and Raman images (Fig. 4, Fig. S6) we could note that red areas were predominantly located on the HeLa cells, with little or no background signals observed in the analysed images, showing the specific attachment of SWNT-AuNPs to cells. At this step of investigation we couldn't speculate on whether the SWNT-AuNPs were stuck to the cell surface or inside the cytoplasm. A more detailed plane by plane in deep Raman analyses are needed and the results will probably elucidate the interaction mechanism of SWNT-AuNPs with cells, taking into account the highly charged negative surface of SWNT-AuNPs due to the attached DNA sequences with cell membrane.

Hybridization experiments

In order to check the possibility of post-synthetic functionalization of the SWNT-AuNPs nanocomposites with the molecules of interest, we conducted a hybridization experiment involving both complementary (positive control) and non-complementary (negative control) single-stranded DNA sequences labeled with a fluorophore (Fig. 5).

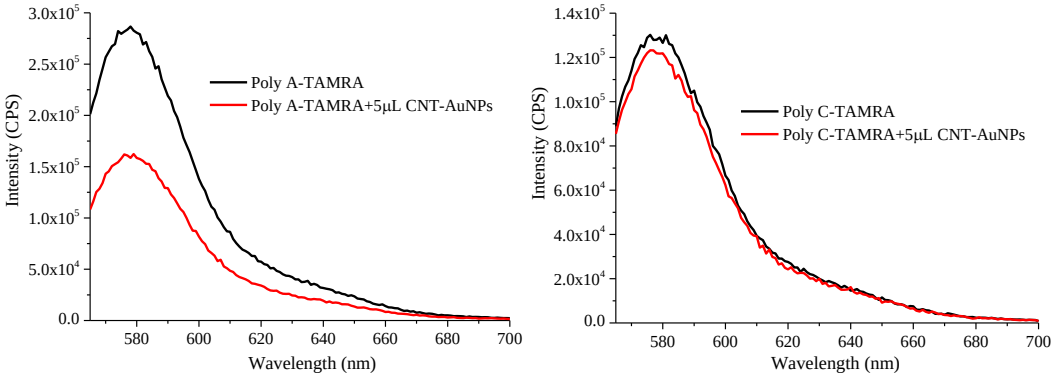

Fig. 5 Fluorescence spectra for the hybridization experiment of the SWNT-AuNPs with complementary 5'-A_{40}-TAMRA-3' (left) and non-complementary 5'-C_{40}-TAMRA-3' (right) sequences.

We have first prepared separate solutions of TAMRA-labeled DNA sequences in 1xTAE buffer (pH = 7.4) and NaCl (0.1 M) with the final volume of 500 µL and measured their fluorescence by exciting at 557 nm (Fig. 5, black curves). The control sequence was designed in such a way that in case of the complementary hybridization with the SWNT-AuNPs the fluorescent molecule should be positioned close to the AuNPs thus considerably quenching its emission (Pal et al. 2013). The length of the TAMRA-labeled sequences was the same as the length of the poly-T sequence attached to the AuNPs. To both investigated solutions a fixed amount (5 µL) of freshly prepared SWNT-AuNPs solution was added and the fluorescence of the resulted mixture was measured (Fig. 5, red curves). The measured emission of the solution where the TAMRA-labeled sequence (poly A-TAMRA) was complementary to the poly-T sequence of the AuNPs attached to the SWNT suffered considerable decrease in intensity (Fig. 5, left). This effect is governed by the binding of the designed complementary strand to the SWNT-AuNPs nanocomposite, showing that a post-synthetic functionalization with chemical modifications able to be attached to a synthetic DNA sequence is possible. The decrease in fluorescence intensity was monitored in course of three hours to complete the hybridization process, hampered by the relatively long complementary sequences. In case of poly C-TAMRA solution (negative control) emission spectra after addition of the same amount of SWNT-AuNPs, did not suffer significant changes (Fig.5, right) after three hours. A small decrease in the spectrum intensity of poly

C-TAMRA after the addition of SWNT-AuNPs could be explained by the unspecific quenching of TAMRA emission by AuNPs in solution.

Conclusions

In summary, a DNA-assisted method has been developed to decorate gold nanoparticles onto pristine SWNTs in the solution phase, yielding SWNT-AuNPs nanocomposites which exhibited noticeable SERS effect. Owing to the strongly enhanced Raman signals of nanotubes by SERS, it was possible to label and Raman image HeLa cells. Moreover, the developed methodology for the preparation of SWNT-AuNPs nanocomposites took into account the possibility of post-synthetic functionalization through complementary hybridization with molecules of interest attached to a complementary DNA strand using well-developed bio-conjugation chemistry. This post-synthetic hybridization possibility was verified by monitoring the quenching of fluorescence signal of TAMRA fluorophore-labeled complementary DNA strand.

The resulted SWNT-AuNPs represent an interesting nanoplatform with easy to tune size of AuNPs prior to the synthesis and facile decoration with large library of small molecules known or easy to attach to synthetic DNA postsynthetically. These make the final nanocomposites promising candidates in selective cancer cell labeling and imaging, nanoscale electronics or sensor developments. Further research towards the increasing the density of AuNPs within the SWNT-AuNPs nanocomposites, possibility of nanocomposite positioning (immobilization) on various surfaces through hybridization or construction of even more complex nanostructures due to available hybridization binding sites are under investigation in our group.

Acknowledgements

This study was funded by a grant of the Romanian National Authority for Scientific Research and Innovation, CNCS – UEFISCDI, project number PN-II-RU-TE-2014-4-1444. The authors are grateful for the financial support from the H2020 WIDESPREAD 2-2014**:** ERA Chairs Project no 667387: SupraChem Lab Laboratory of Supramolecular Chemistry for Adaptive Delivery Systems ERA Chair initiative. The authors declare that they have no conflict of interest.

Notes and references

Azamian BR, Coleman KS, Davis JJ, Hanson N, Green MLH (2002) Directly observed covalent coupling of quantum dots to single-wall carbon nanotubes. Chem Commun, 4:366-367. doi: 10.1039/B110690B

Bartelmess J, Quinn SJ, Giordani S (2015) Carbon nanomaterials: multi-functional agents for biomedical fluorescence and Raman imaging. Chem Soc Rev 44:4672-4698. doi: 10.1039/c4cs00306c

Bartelmess J, Quinn SJ, Giordani S (2015) Carbon nanomaterials: multi-functional agents for biomedical fluorescence and Raman imaging. Chem Soc Rev 44:4672-4698. doi: 10.1039/C4CS00306C

Beqa L, Singh AK, Fan Z, Senapati D, Ray PC (2011) Chemically attached gold nanoparticles carbon nanotube hybrids for highly sensitive SERS substrate. Chem Phys Lett 512:237-242. doi: 10.1016/j.cplett.2011.07.037

Camargo PHC, Au L, Rycenga M, Li W, Xia Y (2010) Measuring the SERS enhancement factors of dimers with different structures constructed from silver nanocubes. Chem Phys Lett 484:304-308. doi: 10.1016/j.cplett.2009.12.002

Cao YC, Jin R, Mirkin CA (2002) Nanoparticles with Raman spectroscopic fingerprints for DNA and RNA detection. Science 297:1536-1540. doi: 10.1126/science.297.5586.1536

Chen Z, Tabakman SM, Goodwin AP, Kattah MG, Daranciang D, Wang X, Zhang G, Li X, Liu Z, Utz P, Jiang K, Fan S, Dai H (2008) Protein microarrays with carbon nanotubes as multicolor Raman labels. Nat. Biotechnol 26:1285-1292. doi: 10.1038/nbt.1501

Choi HC, Shim M, Bangsaruntip S, Dai H (2002) Spontaneous reduction of metal ions on the sidewalls of carbon nanotubes. J Am Chem Soc 124:9058-9059. doi: 10.1021/ja026824t

Chu H, Wei L, Cui R, Wang J, Li Y (2010) Carbon nanotubes combined with inorganic nanomaterials: Preparations and applications. Coordin ChemRev 254:1117-1134. doi: 10.1016/j.ccr.2010.02.009

Ding BQ, Deng ZT, Yan H, Cabrini S, Zuckermann RN, Bokor J (2010) Gold nanoparticle self-similar chain structure organized by DNA origami. J Am Chem Soc 132:3248-3249. doi: 10.1021/ja9101198

Han X, Li Y, Deng Z (2007) DNA-wrapped single walled carbon nanotubes as rigid templates for assembling linear gold nanoparticle arrays. Adv Mater 19:1518-1522. doi: 10.1002/adma.200602861

Heller DA, Baik S, Eurell TE, Strano MS (2005) Single-Walled Carbon Nanotube Spectroscopy in Live Cells: Towards Long-Term Labels and Optical Sensors. Adv Mater 17:2793-2799. doi: 10.1002/adma.200500477

Kam N, Liu Z, Dai H (2005) Functionalization of Carbon Nanotubes via Cleavable Disulfide Bonds for Efficient Intracellular Delivery of siRNA and Potent Gene Silencing. J Am Chem Soc 127:12492-12493. doi: 10.1021/ja053962k

Krafft C, Schie IW, Meyer T, Schmitt M, Popp J (2016) Developments in spontaneous and coherent Raman scattering microscopic imaging for biomedical applications. Chem Soc Rev 45:1819-1849. doi: 10.1039/C5CS00564G

Li Y, Han X, Deng Z (2007) Grafting single-walled carbon nanotubes with highly hybridizable DNA sequences: potential building blocks for DNA-programmed material assembly. Angew Chem Int Ed 46:7481-7484. doi: 10.1002/anie.200701748

Liu X, Tao H, Yang K, Zhang S, Lee ST, Liu Z (2011) Optimization of surface chemistry on single-walled carbon nanotubes for in vivo photothermal ablation of tumors. Biomaterials 32:144-151. doi: 10.1016/j.biomaterials.2010.08.096.

Liu Z, Li X, Tabakman S, Jiang K, Fan S, Dai H (2008) Multiplexed multicolor Raman imaging of live cells with isotopically modified single walled carbon nanotubes. J Am Chem Soc 130:13540-13541. doi: 10.1021/ja806242t

Liu Z, Yang K, Lee ST (2011) Single-walled carbon nanotubes in biomedical imaging. J Mater Chem 21:586-598. doi: 10.1039/C0JM02020F

Meng L, Xia W, Liu L, Niu L, Lu Q (2014) Golden single-walled carbon nanotubes prepared using double layer polysaccharides bridge for photothermal therapy. ACS Appl Mater Interfaces 6:4989-4996. doi: 10.1021/am406031n

Moghaddam MJ, Taylor S, Gao M, Huang S, Dai L, McCall MJ (2004) Highly efficient binding of DNA on the sidewalls and tips of carbon nanotubes using photochemistry. Nano Lett4:89-93. doi: 10.1021/nl034915y

Pal S, Dutta P, Wang H, Deng Z, Zou S, Yan H, Liu Y (2013) Quantum efficiency modification of organic fluorophores using gold nanoparticles on DNA origami scaffolds. J Phys Chem C 117:12735-12744. doi: 10.1021/jp312422n

Polte J, Ahner TT, Delissen F, Sokolov S, Emmerling F, Thünemann AF, Kraehnert R (2010) Mechanism of gold nanoparticle formation in the classical citrate synthesis method derived from coupled in situ XANES and SAXS evaluation. J Am Chem Soc 132:1296-1301. doi: 10.1021/ja906506j

Qian X, Peng XH, Ansari DO, Yin-Goen Q, Chen GZ, Shin DM, Yang L, Young AN, Wang MD, Nie S (2008) In vivo tumor targeting and spectroscopic detection with surface-enhanced Raman nanoparticle tags. Nat Biotechnol 26:83-90. doi:10.1038/nbt1377

Quinn BM, Dekker C, Lemay SG (2005) Electrodeposition of noble metal nanoparticles on carbon nanotubes. J Am Chem Soc 127:6146–6147. doi: 10.1021/ja0508828

Rao AM, Richter E, Bandow S, Chase B, Eklund PC., Williams KA, Fang S, Subbaswamy KR, Menon M, Thess A, Smalley RE, Dresselhaus G, Dresselhaus MS (1997) Diameter-Selective Raman

Scattering from Vibrational Modes in Carbon Nanotubes. Science, 275:187-191. doi: 10.1126/science.275.5297.187

Schoeppler F, Mann C, Hain TC, Neubauer FM, Privitera G, Bonaccorso F, Chu D, Ferrari AC, Hertel T (2011) Molar Extinction Coefficient of Single-Wall Carbon Nanotubes. J Phys Chem C 115: 14682-14686. doi: 10.1021/jp205289h

Turkevich J, Stevenson PC, Hillier J (1951) A study of the nucleation and growth processes in the synthesis of colloidal gold. Discuss Faraday Soc 11:55-75. doi: 10.1039/DF9511100055

Wang X, Wang C, Cheng L, Lee ST, Liu Z (2012) Noble metal coated single-walled carbon nanotubes for applications in surface enhanced Raman scattering imaging and photothermal therapy. J Am Chem Soc 134:7414-7422. doi: 10.1021/ja300140c

Yang W, Ratinac KR, Ringer SP, Thordarson P, Gooding JJ, Braet F (2010) Carbon nanomaterials in biosensors: should you use nanotubes or graphene? Angew Chem Int Ed Engl 49:2114-2138. doi: 10.1002/anie.200903463

Zavaleta CL, Smith BR, Walton I, Doering W, Davis G, Shojaei B, Natan MJ, Gambhir SS (2009) Multiplexed imaging of surface enhanced Raman scattering nanotags in living mice using noninvasive Raman spectroscopy. Proc Natl Acad Sci USA 106:13511-13516. doi: 10.1073/pnas.0813327106